

First Measurement of Transferred Polarization in the Exclusive $\vec{e}p \rightarrow e'K^+\bar{\Lambda}$ Reaction

D.S. Carman,¹ K. Joo,^{2,3} M.D. Mestayer,² B.A. Raue,^{4,2} G. Adams,³¹ P. Ambrozewicz,⁴ E. Anciant,⁶ M. Anghinolfi,¹⁹ D.S. Armstrong,³⁷ B. Asavapibhop,²⁵ G. Audit,⁶ T. Auger,⁶ H. Avakian,¹⁸ H. Bagdasaryan,³⁸ J.P. Ball,⁵ S.P. Barrow,¹⁴ M. Battaglieri,¹⁹ K. Beard,²² M. Bektasoglu,^{29,1} M. Bellis,³¹ C. Bennhold,¹⁵ N. Bianchi,¹⁸ A.S. Biselli,³¹ S. Boiarinov,²¹ B.E. Bonner,³² S. Bouchigny,^{20,2} R. Bradford,⁸ D. Branford,¹³ W.J. Briscoe,¹⁵ W.K. Brooks,² V.D. Burkert,² C. Butuceanu,³⁷ J.R. Calarco,²⁷ B. Carnahan,⁹ A. Cazes,³⁴ C. Cetina,¹⁵ L. Ciciani,²⁹ R. Clark,⁸ P.L. Cole,^{35,2} A. Coleman,³⁷ D. Cords,² P. Corvisiero,¹⁹ D. Crabb,³ H. Crannell,⁹ J.P. Cummings,³¹ E. DeSanctis,¹⁸ P.V. Degtyarenko,² H. Denizli,³⁰ L. Dennis,¹⁴ R. DeVita,¹⁹ K.V. Dharmawardane,²⁹ K.S. Dhuga,¹⁵ C. Djalali,³⁴ G.E. Dodge,²⁹ D. Doughty,^{10,2} P. Dragovitsch,¹⁴ M. Dugger,⁵ S. Dytman,³⁰ O.P. Dzyubak,³⁴ M. Eckhause,³⁷ H. Egiyan,³⁷ K.S. Egiyan,³⁸ L. Elouadrhiri,^{10,2} A. Empl,³¹ P. Eugenio,¹⁴ R. Fatemi,³ G. Fedotov,²⁶ R.J. Feuerbach,⁸ J. Ficenec,³⁶ T.A. Forest,²⁹ H. Funsten,³⁷ S.J. Gaff,¹² M. Gai,¹¹ M. Garçon,⁶ G. Gavalian,^{27,38} S. Gilad,²⁴ G.P. Gilfoyle,³³ K.L. Giovanetti,²² P. Girard,³⁴ E. Golovach,²⁶ C.I.O. Gordon,¹⁶ K. Griffioen,³⁷ S. Grimes,¹ M. Guidal,²⁰ M. Guillo,³⁴ L. Guo,² V. Gyurjyan,² C. Hadjidakis,²⁰ R.S. Hakobyan,⁹ J. Hardie,^{10,2} D. Heddle,^{2,10} P. Heimberg,¹⁵ F.W. Hersman,²⁷ K. Hicks,¹ R.S. Hicks,²⁵ M. Holtrop,²⁷ J. Hu,³¹ C.E. Hyde-Wright,²⁹ B. Ishkhanov,²⁶ M.M. Ito,² D. Jenkins,³⁶ J.H. Kelley,¹² J.D. Kellie,¹⁶ M. Khandaker,²⁸ K.Y. Kim,³⁰ K. Kim,²³ W. Kim,²³ A. Klein,²⁹ F.J. Klein,^{9,2} A.V. Klimenko,²⁹ M. Klusman,³¹ M. Kossov,²¹ L.H. Kramer,^{4,2} Y. Kuang,³⁷ S.E. Kuhn,²⁹ J. Kuhn,³¹ J. Lachniet,⁸ J.M. Laget,⁶ D. Lawrence,²⁵ J. Li,³¹ K. Livingston,¹⁶ A. Longhi,⁹ K. Lukashin,² J.J. Manak,² C. Marchand,⁶ T. Mart,^{17,15} S. McAleer,¹⁴ J. McCarthy,³ J.W.C. McNabb,⁸ B.A. Mecking,² S. Mehrabyan,³⁰ J.J. Melone,¹⁶ C.A. Meyer,⁸ K. Mikhailov,²¹ R. Minehart,³ M. Mirazita,¹⁸ R. Miskimen,²⁵ V. Mokeev,²⁶ L. Morand,⁶ S.A. Morrow,²⁰ M.U. Mozer,¹ V. Muccifora,¹⁸ J. Mueller,³⁰ L.Y. Murphy,¹⁵ G.S. Mutchler,³² J. Napolitano,³¹ R. Nasseripour,⁴ S.O. Nelson,¹² S. Niccolai,¹⁵ G. Niculescu,¹ I. Niculescu,¹⁵ B.B. Niczyporuk,² R.A. Niyazov,²⁹ M. Nozar,^{2,28} G.V. O'Rielly,¹⁵ A.K. Opper,¹ M. Osipenko,²⁶ K. Park,²³ K. Paschke,⁸ E. Pasyuk,⁵ G. Peterson,²⁵ N. Pivnyuk,²¹ D. Pocanic,³ O. Pogorelko,²¹ E. Polli,¹⁸ S. Pozdniakov,²¹ B.M. Preedom,³⁴ J.W. Price,⁷ Y. Prok,³ D. Protopopescu,²⁷ L.M. Qin,²⁹ G. Riccardi,¹⁴ G. Ricco,¹⁹ M. Ripani,¹⁹ B.G. Ritchie,⁵ F. Ronchetti,¹⁸ P. Rossi,¹⁸ D. Rowntree,²⁴ P.D. Rubin,³³ F. Sabatié,^{6,29} K. Sabourov,¹² C. Salgado,²⁸ J.P. Santoro,³⁶ V. Sapunenko,¹⁹ R.A. Schumacher,⁸ V.S. Serov,²¹ Y.G. Sharabian,^{2,38} J. Shaw,²⁵ S. Simionatto,¹⁵ A.V. Skabelin,²⁴ E.S. Smith,² L.C. Smith,³ D.I. Sober,⁹ M. Spraker,¹² A. Stavinsky,²¹ S. Stepanyan,^{29,2} P. Stoler,³¹ M. Taiuti,¹⁹ S. Taylor,³² D.J. Tedeschi,³⁴ U. Thoma,² R. Thompson,³⁰ L. Todor,⁸ C. Tur,³⁴ M. Ungaro,³¹ M.F. Vineyard,³³ A.V. Vlassov,²¹ K. Wang,³ L.B. Weinstein,²⁹ H. Weller,¹² D.P. Weygand,² C.S. Whisnant,³⁴ E. Wolin,² M.H. Wood,³⁴ A. Yegneswaran,² J. Yun,²⁹ B. Zhang,²⁴ J. Zhao,²⁴ Z. Zhou,²⁴

(CLAS collaboration)

¹ Ohio University, Athens, Ohio 45701

² Thomas Jefferson National Accelerator Laboratory, Newport News, Virginia 23606

³ University of Virginia, Charlottesville, Virginia 22901

⁴ Florida International University, Miami, Florida 33199

⁵ Arizona State University, Tempe, Arizona 85287

⁶ CEA-Saclay, DAPNIA-SPhN, F91191 Gif-sur-Yvette Cedex, France

⁷ University of California at Los Angeles, Los Angeles, California 90095

⁸ Carnegie Mellon University, Pittsburgh, Pennsylvania 15213

⁹ Catholic University of America, Washington, D.C. 20064

¹⁰ Christopher Newport University, Newport News, Virginia 23606

¹¹ University of Connecticut, Storrs, Connecticut 06269

¹² Duke University, Durham, North Carolina 27708

¹³ Edinburgh University, Edinburgh EH9 3JZ, United Kingdom

¹⁴ Florida State University, Tallahassee, Florida 32306

¹⁵ The George Washington University, Washington, DC 20052

¹⁶ University of Glasgow, Glasgow G12 8QQ, United Kingdom

¹⁷ Jurusan Fisika, FMIPA, Universitas Indonesia, Depok 16424, Indonesia

¹⁸ INFN, Laboratori Nazionali di Frascati, P.O. 13,00044 Frascati, Italy

¹⁹ INFN, Sezione di Genova and Dipartimento di Fisica, Università di Genova, 16146 Genova, Italy

²⁰ Institut de Physique Nucleaire d'ORSAY, IN2P3, BP1, 91406 Orsay, France

²¹ Institute of Theoretical and Experimental Physics, Moscow, 117259, Russia

²² James Madison University, Harrisonburg, Virginia 22807

²³ Kyungpook National University, Daegu 702-701, South Korea

- ²⁴ *Massachusetts Institute of Technology, Cambridge, Massachusetts 02139*
²⁵ *University of Massachusetts, Amherst, Massachusetts 01003*
²⁶ *Moscow State University, 119899 Moscow, Russia*
²⁷ *University of New Hampshire, Durham, New Hampshire 03824*
²⁸ *Norfolk State University, Norfolk, Virginia 23504*
²⁹ *Old Dominion University, Norfolk, Virginia 23529*
³⁰ *University of Pittsburgh, Pittsburgh, Pennsylvania 15260*
³¹ *Rensselaer Polytechnic Institute, Troy, New York 12180*
³² *Rice University, Houston, Texas 77005*
³³ *University of Richmond, Richmond, Virginia 23173*
³⁴ *University of South Carolina, Columbia, South Carolina 29208*
³⁵ *University of Texas at El Paso, El Paso, Texas 79968*
³⁶ *Virginia Polytechnic Institute and State University, Blacksburg, Virginia 24061*
³⁷ *College of William and Mary, Williamsburg, Virginia 23187 and*
³⁸ *Yerevan Physics Institute, 375036 Yerevan, Armenia*

(Dated: November 13, 2018)

The first measurements of the transferred polarization for the exclusive $\bar{e}p \rightarrow e'K^+\bar{\Lambda}$ reaction have been performed in Hall B at the Thomas Jefferson National Accelerator Facility using the CLAS spectrometer. A 2.567 GeV electron beam was used to measure the hyperon polarization over a range of Q^2 from 0.3 to 1.5 (GeV/c)², W from 1.6 to 2.15 GeV, and over the full center-of-mass angular range of the K^+ meson. Comparison with predictions of hydrodynamic models indicates strong sensitivity to the underlying resonance contributions. A non-relativistic quark model interpretation of our data suggests that the $s\bar{s}$ quark pair is produced with spins predominantly anti-aligned. Implications for the validity of the widely used 3P_0 quark-pair creation operator are discussed.

PACS numbers: 13.88.+e, 14.40.aq, 14.20.Gk, 14.20.Jn

We present here the first measurements of spin transfer in the nucleon resonance region from a longitudinally polarized electron beam to the Λ hyperon produced in the exclusive $p(\bar{e}, e'K^+)\bar{\Lambda}$ reaction. Understanding nucleon resonance excitation continues to provide a major challenge to hadronic physics due to the non-perturbative nature of QCD at these energies. Studies of strange final states have the potential to uncover baryonic resonances that do not couple or couple only weakly to the πN channel due to the different hadronic vertices. Recent symmetric quark-model calculations predict more states than have been found experimentally [1]. The issue of whether these missing resonances do in fact exist is directly tied to the question of whether certain quark degrees of freedom might be “frozen out” as in, e.g., certain diquark models [2]. This question is central to our understanding of baryon structure.

In the absence of direct QCD predictions, the theoretical framework involving hydrodynamic models has been extensively applied to the study of electromagnetic production of pseudoscalar mesons [3, 4, 5, 6]. Considerable effort over the last two decades has been expended to develop these effective Lagrangian models; however, their predictive powers are still limited by a sparsity of data. Model fits to the existing cross section data are generally obtained at the expense of many free parameters, and these unpolarized data alone are not sufficiently sensitive to fully understand the reaction mechanism as they probe only a small portion of the full response. Our double-polarization data can provide significant new constraints on the basic parameters of these models, increasing their discriminatory power and allowing for a quan-

titative measure of whether or not new “missing” resonances might be required to explain these and other hyperon production data.

Alternatively, our data provide interesting, and perhaps surprising, information about the nature of quark-pair production. There is a growing body of evidence that the appropriate degrees of freedom to describe the phenomenology of hadronic decays are constituent quarks held together by a gluonic flux-tube [7]. The non-perturbative nature of the flux-tube gives rise to the well-known linear potential of heavy-quark confinement ($dV/dr \sim 1$ GeV/fm) [8]. Other properties of the flux-tube can be determined by studying $q\bar{q}$ pair production, since this is widely believed to produce the color field neutralization that actually breaks the flux-tube. Since the suggestions in the 1970’s that a quark pair with vacuum quantum numbers is responsible for breaking the color flux-tube (the 3P_0 model [9]), theorists have used increasingly sophisticated and realistic models to understand the experimental data [10, 11].

The most sensitive experimental tests to date have measured the ratio of strong amplitudes differing in their orbital angular momenta in certain meson decays [11]. Since the 3P_0 operator has $S=1$ and $L=1$, it implies a different amplitude ratio than, e.g., a 3S_1 operator with $S=1$ and $L=0$, corresponding to one gluon exchange. Later, we will argue that the spin properties of the quark-pair creation operator might be responsible for the observed trends in the Λ polarization. Furthermore, by analogy of an argument used to explain the observed transverse polarization of Λ hyperons in exclusive $pp \rightarrow pK^+\Lambda$ [12], we conclude that the relevant quark-pair creation oper-

ator dominating our reaction produces the $s\bar{s}$ pair with spins anti-aligned. This finding, if confirmed by further calculations, brings into question the universal applicability of the 3P_0 model. This has important implications since many, if not most, calculations of hadronic spectroscopy use the 3P_0 operator to calculate the transition to the final-state particles [13].

The Continuous Electron Beam Accelerator Facility (CEBAF) at Jefferson Laboratory provides multi-GeV electron beams with longitudinal polarization up to 80%. In Hall B of this facility is the CEBAF Large Acceptance Spectrometer (CLAS) [14], a detector constructed around six superconducting coils that generate a toroidal magnetic field to momentum-analyze charged particles. The detection system consists of multiple layers of drift chambers to determine charged-particle trajectories, Čerenkov detectors for electron/pion separation, scintillation counters for flight-time measurements, and calorimeters to identify electrons and high-energy neutral particles. Operating luminosity with the unpolarized liquid- H_2 target is $\sim 1 \times 10^{34} \text{ cm}^{-2} \text{ sec}^{-1}$.

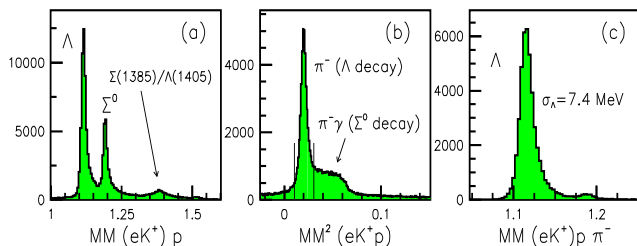


FIG. 1: Missing-mass spectra (GeV) for the reactions (a) $p(e, e'K^+)X$ and (b) $p(e, e'K^+p)X$. (c) The hyperon distribution after cutting on the low-mass peak in (b). Data from 2.567 GeV CLAS data summing over all Q^2 and W .

The large acceptance of CLAS has enabled us to detect the final-state electron and kaon, and the proton from the decay of the Λ hyperon at a beam energy of 2.567 GeV, over a range of momentum transfer Q^2 from 0.3 to 1.5 $(\text{GeV}/c)^2$ and invariant energy W from 1.6 to 2.15 GeV, while providing full angular coverage in the kaon center-of-mass (CM). Hyperon identification with CLAS relies on missing-mass reconstructions. Fig. 1a shows the missing-mass for $p(e, e'K^+)X$ where a proton has also been detected. Fig. 1b shows the missing mass for $p(e, e'K^+p)X$, where the final-state proton can come from the decay of the $\Lambda(1115)$ (missing π^-) or the $\Sigma^0(1192)$ (missing $\pi^- \gamma$). Fig. 1c shows the resulting hyperon spectrum after a cut on the π^- peak in Fig. 1b.

An attractive feature of the mesonic decay $\Lambda \rightarrow p\pi^-$ comes from its self-analyzing nature. This weak decay has an asymmetric angular distribution with respect to the Λ spin direction due to an interference between parity non-conserving (s -wave) and parity-conserving (p -wave) amplitudes. The decay-proton distribution in the Λ rest frame (RF) for each beam helicity state is of the form:

$$\frac{dN^\pm}{d\cos\theta_p^{RF}} = N[1 + \alpha(P^0 \pm P_b P') \cos\theta_p^{RF}], \quad (1)$$

where P_b is the average beam polarization and $\alpha=0.642 \pm 0.013$ is the weak decay asymmetry parameter [15]. The Λ polarization is the sum of P^0 , the induced polarization, and P' , the helicity-dependent transferred polarization, both defined with respect to a particular set of spin-quantization axes. This latter quantity is the focus of this work. Fig. 2 highlights two standard choices for the spin-quantization axes defined in relation to the electron and hadron reaction planes.

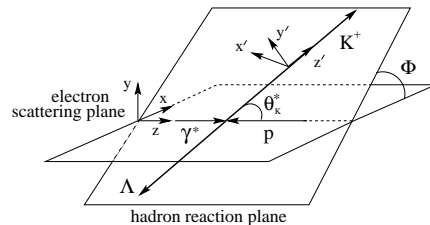


FIG. 2: Center-of-mass coordinate system highlighting the definitions of the different spin-quantization axis choices for the final-state Λ hyperon used in the polarization analysis.

Using eq.(1), we can express the acceptance-corrected yield asymmetries in terms of the average transferred polarization for each kinematic bin as:

$$A_\xi(\cos\theta_p^{RF}) = \frac{N_\xi^+ - N_\xi^-}{N_\xi^+ + N_\xi^-} = \frac{\alpha P_b \cos\theta_p^{RF} P'_\xi}{1 + \alpha P_\xi^0 \cos\theta_p^{RF}}. \quad (2)$$

Here $N_\xi^\pm(\cos\theta_p^{RF})$ are the decay-proton helicity-gated yields with respect to the different spin-quantization axes $\xi = \hat{i}, \hat{j}, \hat{k}$. Using this method we are quite insensitive to the form of the CLAS acceptance function.

Using the notation of Ref. [16], the most general form for the virtual photo-absorption CM cross section for the $p(\bar{e}, e'K^+)\bar{\Lambda}$ reaction from an unpolarized proton target, allowing for both a polarized-electron beam and recoil hyperon is given by:

$$\begin{aligned} \frac{d\sigma_v}{d\Omega_K^*} = \mathcal{K} \sum_{\beta=0, x', y', z'} & \left(R_T^{\beta 0} + \epsilon_L R_L^{\beta 0} + c_+ ({}^c R_{LT}^{\beta 0} \cos\Phi \right. \\ & + {}^s R_{LT}^{\beta 0} \sin\Phi) + \epsilon ({}^c R_{TT}^{\beta 0} \cos 2\Phi + {}^s R_{TT}^{\beta 0} \sin 2\Phi) \\ & \left. + P_b c_- ({}^c R_{LT'}^{\beta 0} \cos\Phi + {}^s R_{LT'}^{\beta 0} \sin\Phi) + P_b c_0 R_{TT'}^{\beta 0} \right). \quad (3) \end{aligned}$$

The R_i are the transverse, longitudinal, and interference response functions that relate to the underlying hadronic current and implicitly contain the Λ polarization. The sum over β includes contributions from the polarization with respect to the (x', y', z') axes (see Fig. 2), and the $\beta = 0$ terms account for the unpolarized response. Here $c_\pm = \sqrt{2\epsilon_L(1 \pm \epsilon)}$ and $c_0 = \sqrt{1 - \epsilon^2}$, where ϵ ($\epsilon_L = \epsilon Q^2 / (k_\gamma^{CM})^2$) is the transverse (longitudinal) polarization of the virtual photon, $\mathcal{K} = |\vec{q}_K| / k_\gamma^{CM}$, and Φ is the angle between the electron and hadron planes. The c and s labels indicate whether R_i multiplies a sine or cosine term.

From the cross section of eq.(3), the induced and transferred polarization components in the (x', y', z') system are given by [17]:

$$\begin{aligned}\sigma_0 P_\xi^0 &= \mathcal{K}(c_+ R_{LT}^{\xi 0} \sin \Phi + \epsilon R_{TT}^{\xi 0} \sin 2\Phi), \quad \xi = x', z' \quad (4) \\ \sigma_0 P_{y'}^0 &= \mathcal{K}(R_T^{y'0} + \epsilon_L R_L^{y'0} + c_+ R_{LT}^{y'0} \cos \Phi + \epsilon R_{TT}^{y'0} \cos 2\Phi) \\ \sigma_0 P_\xi' &= \mathcal{K}(c_- R_{LT'}^{\xi 0} \cos \Phi + c_0 R_{TT'}^{\xi 0}), \quad \xi = x', z' \\ \sigma_0 P_{y'}' &= \mathcal{K} c_- R_{LT'}^{y'0} \sin \Phi\end{aligned}\quad (5)$$

Here σ_0 is the unpolarized cross section. These definitions can be related to the (x, y, z) system via appropriate rotation operators.

The data were summed over all Φ angles to improve the statistical precision in the measurement. In the summation, the induced components $P_{x', z'}^0$ and $P_{x, z}^0$, and the transferred components $P_{y'}^0$ and P_y^0 , vanish identically. In this case, the non-zero, helicity-gated yield asymmetries of eq.(2) reduce to:

$$A_\xi = \alpha P_b \cos \theta_p^{RF} P_\xi', \quad \xi = \hat{i}, \hat{k}, \quad (6)$$

allowing for a direct extraction of P' in a given kinematic bin with a linear fit of A_ξ to $\cos \theta_p^{RF}$. Note that different choices for the spin axes lead to sensitivities of P' to different subsets of the response functions. The non-zero, Φ -integrated transferred polarization components in the (x', y', z') and (x, y, z) systems are given by:

$$\begin{aligned}P_{x'}' &= c_1 R_{TT'}^{x'0} & P_{z'}' &= c_1 R_{TT'}^{z'0} \\ P_x' &= c_2 (R_{LT'}^{x'0} \cos \theta_K^* - R_{LT'}^{y'0} + R_{LT'}^{z'0} \sin \theta_K^*) \\ P_z' &= c_1 (-R_{TT'}^{x'0} \sin \theta_K^* + R_{TT'}^{z'0} \cos \theta_K^*).\end{aligned}\quad (7)$$

The normalization factors are given by $c_1 = c_0/K_0$ and $c_2 = c_-/(2K_0)$, where $K_0 = R_T^{00} + \epsilon_L R_L^{00}$. This formalism is important to highlight as the hydrodynamic models provide the response functions in the (x', y', z') system as their outputs.

Our results are shown in Figs. 3 and 4 compared to several hydrodynamic model calculations. The error bars in these figures include statistical but not systematic uncertainties, which we estimate to be ≤ 0.08 on the polarization [19]. Fig. 3 shows the W dependence of P' summed over all Q^2 and $d\Omega_K^*$ for our two choices of spin axes. The data indicate sizeable Λ polarizations with a relatively smooth variation with W . The average polarization magnitude is roughly the same along the z' and x' axes, indicating equal strength in the $R_{TT'}^{z'0}$ and $R_{TT'}^{x'0}$ responses. For the other choice of axes, the polarization is maximal when projected along the z -axis (the virtual photon direction), while the component along the x -axis is consistent with zero.

Fig. 4 shows the angular dependence of P' summed over all Q^2 for three different W bins from just above threshold to 2 GeV. The polarization $P_{z'}'$ decreases with increasing θ_K^* . $P_{x'}'$ is constrained to be zero at $\cos \theta_K^* = \pm 1$ due to angular momentum conservation, and reaches

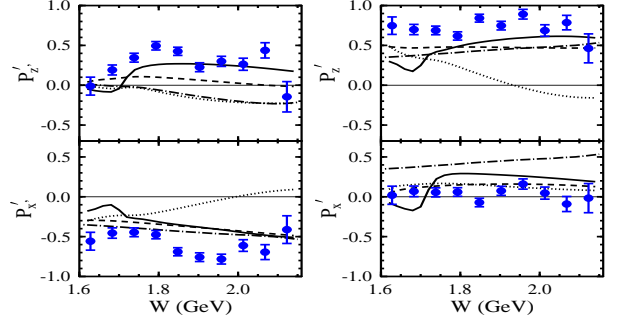


FIG. 3: Transferred Λ polarization components $P_{z'}'$ and $P_{x'}'$ (left) and P_z' and P_x' (right) at 2.567 GeV vs. W (GeV) summed over all Q^2 and $d\Omega_K^*$. Curves correspond to the hydrodynamic models: WJC92 (dotted), BM98 (dashed), BM02 (solid), J02 (dot-dash), averaged over the experimental bins.

a minimum at $\theta_K^* \sim 90^\circ$. Again, the maximum Λ polarization occurs along the virtual photon direction. This component, $P_{z'}'$, is roughly constant with respect to $\cos \theta_K^*$ and W . The component $P_{x'}'$ in the electron-scattering plane is again consistent with zero. The components $P_{y'}'$ and P_y' (not shown) are statistically consistent with zero with respect to W and $\cos \theta_K^*$ as expected [19].

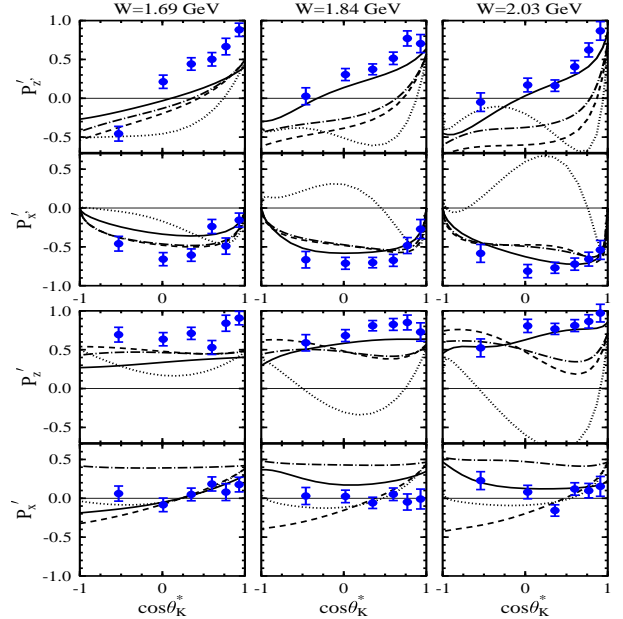


FIG. 4: Transferred Λ polarization components $P_{z'}'$ and $P_{x'}'$ (upper) and P_z' and P_x' (lower) at 2.567 GeV vs. $\cos \theta_K^*$ summed over all Q^2 and Φ for three W bins centered at 1.69, 1.84, and 2.03 GeV. The curves are the same as Fig. 3.

In each of the hydrodynamic models to which we compare our data, the coupling strengths have been determined by a simultaneous fit to the low-energy $K^- p \rightarrow \gamma Y$ radiative capture data and/or $\gamma^{(*)} p \rightarrow K^+ Y$ data, by adding the non-resonant Born terms with a number of resonances and leaving their coupling constants as free

parameters bounded loosely by SU(3) predictions. Different models have markedly different ingredients and fitted coupling constants. In all cases, good agreement with the limited previous data has been achieved [3, 4, 5, 6]. The comparison of the models to data can be used to provide indirect support for the existence of these excited states and their branching ratios into the strange channels.

Resonance	WJC92	BM98	BM02	J02
$N^*(1650), N^*(1710)$	*	*	*	*
$N^*(1720)$			*	*
$N^*(1895)$			*	*
$K^*(892)$	*	*	*	*
$K_1(1270)$	*		*	*
$\Lambda^*(1405)$	*			
$\Lambda^*(1800), \Lambda^*(1810)$				*

TABLE I: Resonances included in the hadrodynamical models highlighted in this work included with the non-resonant Born terms. References to the models can be found in the text.

Recent calculations have been guided by coupled-channels analyses [18, 20] that recognize the importance of the $S_{11}(1650)$, $P_{11}(1710)$, and $P_{13}(1720)$ s -channel resonances, which are also the only ones with a known significant branching into the strange channels [15]. The $p(e, e'K^+)\Lambda$ cross section data exhibit a forward peaking in θ_K^* that has been attributed to t -channel exchanges [21]. For this reason the two lowest vector meson resonances $K^*(892)$ and $K_1(1270)$ are also typically included. A comparison of the four different models employed in this work is included in Table I. These models were developed by Williams, Ji, and Cotanch (WJC92) [3], Bennhold and Mart (BM02, BM98) [4, 22], and Janssen (J02) [6]. These models differ in their mix of N^* resonances, e.g. BM02 and J02 both include one of the missing quark-model states, the $D_{13}(1895)$. Some of the models include Y^* resonances in the u channel, and the most recent models (all but WJC92) have included form factors at the hadronic vertices. In this work, we have employed simple electromagnetic dipole form factors for the kaon and the hyperon.

The calculations generally do not reproduce the data in Figs. 3 and 4, however, the BM02 model best reflects the data. It should be noted that the kink at $W \sim 1.7$ GeV in the BM02 model implies a problem with modeling of the form factors of either the $P_{11}(1710)$ or the $P_{13}(1720)$ states. While the comparison of the calculations to the data is illustrative to highlight the present deficiencies in the current models and their parameter values, the next step in the study of the reaction mechanism is to include our polarization data in the available database and to refit the set of coupling strengths.

As noted earlier, our data reveal a simple phenomenology that indicates the Λ polarization is maximal along the virtual photon direction. We note that the lack of a strong W dependence is an indication that the data

might be economically described in a flux-tube strong-decay framework. In this picture we expect that the cross section is dominated by photo-absorption by a u quark. When viewed in the γ^*-p Breit frame, after a u quark has absorbed the virtual photon, there is an intermediate u -(ud) system with the u quark polarized along the photon direction ($+z$) due to the helicity-conserving vector interaction. Hadronization into the $K^+-\Lambda$ final state proceeds with the production of an $s\bar{s}$ pair that breaks the color flux-tube. Because the u quark hadronizes as a pseudoscalar K^+ , the \bar{s} quark spin is required to be opposite to that of the u quark, i.e. in the $-z$ direction. In the non-relativistic quark model the entire spin of the Λ is carried by the s quark (this assumption has been questioned in light of the NMC “spin crisis” [23]). Since we observe the Λ polarization to be in the $+z$ direction, we conclude that the s and \bar{s} spins were anti-aligned when they were created, if the hadronization did not flip or rotate their spins. We note that the authors of Ref. [12] also posit a two-step process for the production of transversely polarized Λ hyperons in the exclusive $pp \rightarrow pK^+\Lambda$ reaction, and come to the similar conclusion that the s and \bar{s} quark pair must also have been produced with spins anti-aligned.

A dominance of spin anti-alignment for the s and \bar{s} quarks is not consistent with the $S=1$ 3P_0 operator, which predicts a 2:1 mixture of $s\bar{s}$ quarks produced with spins aligned vs. anti-aligned if the orbital substates are equally populated. Along with other observations of failure of the 3P_0 model (e.g. explaining $\pi_2 \rightarrow \rho\omega$ decay [13]), the applicability of the 3P_0 model in describing all hadronic decays is brought into doubt. We await theoretical investigations on the effect of the functional form of the quark-pair-creation operator on hyperon polarizations when a single $s\bar{s}$ pair is produced.

We have reported the first double-polarization measurements in the resonance region for the $p(\vec{e}, e'K^+)\Lambda$ reaction. Our data show a large degree of Λ polarization, which is maximal along the virtual photon direction (averaging $\sim 75\%$ for our kinematics). As this is the first polarization data set, inclusion into the available database should make hadrodynamical models much more reliable for studies of missing-resonance production. Additionally, we feel that a better handle on the form of the quark-pair creation operator will make baryon spectroscopic models more reliable, hence increasing our confidence in their predictions for missing resonances.

We would like to acknowledge the outstanding efforts of the JLab staff that made this experiment possible. This work was supported in part by the the U.S. Department of Energy and National Science Foundation, the Istituto Nazionale di Fisica Nucleare, the French Centre National de la Recherche Scientifique, the French Commissariat à l’Energie Atomique, and the Korea Science and Engineering Foundation. The Southeastern Universities Research Association operates JLab for the U.S. Department of Energy under contract DE-AC05-84ER40150.

-
- [1] S. Capstick and W. Roberts, Phys. Rev. D **58**, 74011 (1998).
- [2] R. Alkofer *et al.*, Nucl. Phys. A **680**, 70 (2001).
- [3] R.A. Williams, C.R. Ji, and S.R. Cotanch, Phys. Rev. C **46**, 1617 (1992).
- [4] T. Mart and C. Bennhold, Phys. Rev. C **61**, 012201 (2000).
- [5] B. Saghai, preprint nucl-th/0105001, (2001).
- [6] S. Janssen *et al.*, Phys. Rev. C **65**, 015201 (2002).
- [7] N. Isgur and J. Paton, Phys. Rev. D **31**, 2910 (1985).
- [8] G.S. Bali, C. Schlichter, and K. Schilling, Phys. Rev. D **51**, 5165 (1995).
- [9] A. LeYaouanc *et al.*, Phys. Rev. D **8**, 2223 (1973).
- [10] E.S. Ackleh, T. Barnes, and E.S. Swanson, Phys. Rev. D **54**, 6811 (1996).
- [11] P. Geiger and E.S. Swanson, Phys. Rev. D **50**, 6855 (1994).
- [12] Zuo-tang Liang and C. Boros, Phys. Rev. D **61**, 117503 (2000).
- [13] T. Barnes, HADRON 2001 Conference Summary, preprint hep-ph/0202157, (2002).
- [14] B.A. Mecking *et al.*, to be submitted to Nucl. Inst. and Meth., (2002).
- [15] D.E. Groom *et al.*, Particle Data Group, Eur. Phys. J **15**, 1 (2000).
- [16] G. Knöchlein, D. Drechsel, and L. Tiator, Z. Phys. A **352**, 327 (1995).
- [17] H. Schmieden, Eur. Phys. J **A1**, 427 (1998).
- [18] T. Feuster and U. Mosel, Phys. Rev. C **59**, 460 (1999).
- [19] D.S. Carman and B.A. Raue, CLAS-note 02-018, E99-006 Analysis Document.
- [20] C. Bennhold *et al.*, Proceedings of N*2001, World Scientific, eds. D. Dreschel and L. Tiator, (2001).
- [21] K.H. Hicks, Proceedings of Hadron2001, AIP Conference Proceedings **619**, eds. D. Amelin and A. Zaitsev, (2001).
- [22] H. Haberzettl *et al.*, Phys. Rev. C **58**, R40 (1998).
- [23] M. Burkardt and R.L. Jaffe, Phys. Rev. Lett. **70**, 2537 (1993).